ehp ENVIRONMENTAL HEALTH PERSPECTIVES
http://www.ehponline.org

Physiologically Based Pharmacokinetic (PBPK) Modeling of Interstrain Variability in Trichloroethylene Metabolism in the Mouse

Weihsueh A. Chiu, Jerry L. Campbell Jr., Harvey J. Clewell 3rd, Yi-Hui Zhou, Fred A. Wright, Kathryn Z. Guyton, and Ivan Rusyn

http://dx.doi.org/10.1289/ehp.1307623

Received: 10 September 2013
Accepted: 10 February 2014
Advance Publication: 11 February 2014

NIH National Institute of Environmental Health Sciences

Physiologically Based Pharmacokinetic (PBPK) Modeling of Interstrain Variability in Trichloroethylene Metabolism in the Mouse

Weihsueh A. Chiu,[1] Jerry L. Campbell Jr.,[2] Harvey J. Clewell 3rd,[2] Yi-Hui Zhou,[3] Fred A. Wright,[3] Kathryn Z. Guyton,[1] and Ivan Rusyn[4]

[1]National Center for Environmental Assessment, Office of Research and Development, U.S. Environmental Protection Agency, Washington, DC, USA; [2]The Hamner Institutes for Health Sciences, Research Triangle Park Park, NC, USA; Departments of [3]Biostatistics and [4]Environmental Sciences and Engineering, University of North Carolina, Chapel Hill, NC, USA

Address correspondence to Ivan Rusyn, University of North Carolina. Telephone: 919-843-2596. E-mail: iir@unc.edu; Weihsueh Chiu, US EPA. Telephone : 703-347-8607. E-mail: chiu.weihsueh@epa.gov,

Running Title: Population-based PBPK modeling of TCE in the mouse

Acknowledgments: Supported in part by grants from the NIH: P42 ES005948 (JLC, HJC, Y-HZ, FAW, IR), R01 ES015241 (IR), and P30 ES010126 (IR, FAW). Ivan Rusyn was supported, in part, by the Oak Ridge Institute for Science and Education fellowships made available through funding from the U.S. EPA.

Disclaimer: The views expressed herein do not necessarily represent those of the U.S. EPA.

Competing Financial Interests: None of the authors has any actual or potential competing financial interests.

Abstract

Background: Quantitative estimation of toxicokinetic variability in the human population is a persistent challenge in risk assessment of environmental chemicals. Traditionally, inter-individual differences in the population are accounted for by default assumptions or, in rare cases, are based on human toxicokinetic data.

Objectives: To evaluate the utility of genetically diverse mouse strains for estimating toxicokinetic population variability for risk assessment, using trichloroethylene (TCE) metabolism as a case study.

Methods: We used data on oxidative and glutathione conjugation metabolism of TCE in 16 inbred and one hybrid mouse strains to calibrate and extend existing physiologically-based pharmacokinetic (PBPK) models. We added one-compartment models for glutathione metabolites and a two-compartment model for dichloroacetic acid (DCA). A Bayesian population analysis of interstrain variability was used to quantify variability in TCE metabolism.

Results: Concentration-time profiles for TCE metabolism to oxidative and glutathione conjugation metabolites varied across strains. Median predictions for the metabolic flux through oxidation was less variable (5-fold range) than that through glutathione conjugation (10-fold range). For oxidative metabolites, median predictions of trichloroacetic acid production was less variable (2-fold range) than DCA production (5-fold range), although uncertainty bounds for DCA exceeded the predicted variability.

Conclusions: Population PBPK modeling of genetically diverse mouse strains can provide useful quantitative estimates of toxicokinetic population variability. When extrapolated to lower doses more relevant to environmental exposures, mouse population-derived variability estimates for TCE metabolism closely matched population variability estimates previously derived from

human toxicokinetic studies with TCE, highlighting the utility of mouse interstrain metabolism studies for addressing toxicokinetic variability.

Introduction

TCE is not only an important industrial chemical and a ubiquitous environmental contaminant, but also there are complex scientific issues related to its metabolism, the modes, targets and types of toxicity, and its potential to be a human health hazard. The U.S. Environmental protection Agency (EPA) and the International Agency for Research on Cancer concluded that TCE is carcinogenic to humans (Chiu et al. 2013; Guha et al. 2012). While the cancer hazard classification of TCE has been agreed upon by several expert panels, scientific challenges in the interpretation of the dose-response assessment remain. Major issues include the extent of TCE metabolism through cytochrome P450-mediated oxidation and GST-mediated glutathione conjugation pathways (Lash et al. 2000), and the inter-individual differences in formation of liver- and kidney-toxic metabolites of TCE (Chiu et al. 2009).

Based on the recommendations of the National Research Council (National Research Council 2006), a physiologically-based pharmacokinetic model (PBPK) was used to derive candidate reference dose and concentration values for non-cancer human health effects of TCE. A comprehensive PBPK model of Hack et al. (2006) was updated using the Bayesian framework for estimation and characterization of the PBPK model parameter uncertainties (Chiu et al. 2009; Evans et al. 2009). This model was used for the dose-response assessment in EPA's TCE toxicological review (U.S. EPA 2011), specifically for quantitative dose extrapolation across routes of exposure, across species, and within species. This latter extrapolation – addressing toxicokinetic variability in the human population – was only possible because of the availability of individual human data on TCE toxicokinetics.

Characterizing variability remains a key risk assessment challenge (Zeise et al. 2013), and there are few chemicals for which sufficient individual human toxicokinetic data are available to conduct population PBPK modeling. Even for TCE, the data are limited to healthy male human volunteers, largely of European descent. Furthermore, the data on glutathione conjugation was much more limited, and questions have been raised as to its reliability for making quantitative estimates of the internal dose. While it is unlikely that sufficient additional human toxicokinetic data will become available in the future to refine estimates of human toxicokinetic variability, either for TCE or for other chemicals, new experimental approaches using genetically diverse mouse populations offer a potential alternative for evaluating variability. In fact, interstrain differences in TCE metabolism have been quantified using a multistrain panel of inbred mice (Bradford et al. 2011).

TCE offers an attractive case study for examining the utility of the mouse population for characterizing variability. We show that significant strain and time effects are observed in metabolism of TCE. Next, we calibrated and further refined PBPK models of TCE (Evans et al. 2009; Hack et al. 2006). One-compartment models were added for S-(1,2-dichlorovinyl)glutathione (DCVG) and S-(1,2-dichlorovinyl)-L-cysteine (DCVC), and a two-compartment model for DCA. Finally, a population model for interstrain variability was added to quantify the extent of variability in metabolism through oxidation and glutathione conjugation.

Materials and Methods

Animals, treatments and data availability

Data used for the analyses presented herein were previously reported (Bradford et al. 2011; Kim et al. 2009b). Additional unpublished data from Bradford et al. (2011) study in AKR/J or

WSB/EiJs strains are provided as Supplemental Material, Table S1. Males (aged 7-9 weeks) from these 16 inbred and one hybrid (B6C3F1/J) mouse strains (Jackson Laboratory, Bar Harbor, ME) were gavaged with TCE (2100 mg/kg) in corn oil (10 ml/kg) and sacrificed at 2, 8 and 24 hrs after treatment. Concentrations of DCA, TCA, DCVG and DCVC in mouse serum were determined as detailed in (Bradford et al. 2011; Kim et al. 2009a). All studies were conducted with approval of the Institutional Animal Care and Use Committee, the animals were treated humanely and with regard for alleviation of suffering.

Analysis of variance (ANOVA) modeling of strain and time effects on concentration-time profiles of TCE metabolites in mouse serum

Individual animal-level serum TCE metabolite data was examined in a series of power transformations across a grid from 0 (the log transformation) to 1 (untransformed). The transformation y_new=y^0.25 produced the closest average fit to normality across the metabolites, with no influential outliers. Histograms of the transformed values and quantile-quantile plots for each TCE metabolite are shown in Supplemental Material, Figure S1.

Analysis of variance (ANOVA) models were fit to the data for strain as a factor within each time point, and with strain and time point as factors in an overall model, with time point added first to the ANOVA model. An approximate "heritability" was computed as the portion of variation attributable to strain, which was determined using the partial R^2. Statistical tests involving each metabolite were treated as separate hypotheses of independent interest, and thus not subjected to multiple comparison control.

Monte Carlo analysis of concentration-time profiles of TCE metabolites in mouse serum

Monte Carlo analysis of the data was carried out using the TCE PBPK model (Hack et al. 2006) with slight modifications (Supplemental Material, Figure S2). The model was modified to incorporate production of DCVG. DCVG clearance was described as metabolism to DCVC. The production of DCA was also altered. In the original model (Hack et al. 2006), DCA was only the product of direct metabolism of TCE. In the modified model, DCA is the product of both direct metabolism of TCE, as well from the enzymatic dehalogenation of TCA (Kim et al. 2009b). Model parameters are given in Supplemental Material, Table S2. All other parameters were fixed to the mean posterior value reported in (Hack et al. 2006). Monte Carlo analysis was carried out by varying the metabolism and excretion of TCE, TCA, DCA, DCVG and DCVC while holding all other parameters constant (an approach supported by a sensitivity analysis, discussed later, that confirmed the lack of sensitivity of PBPK model calibration to these parameters). Values for the metabolism were generated randomly from a normal distribution in acslX (Aegis Technologies, Huntsville, AL). The Monte Carlo simulation was run for 100 iterations.

Model refinement and Bayesian approach to estimating interstrain variability in concentration-time profiles of TCE metabolites in mouse serum

After completing the preliminary analysis, the additional DCVG, DCVC, and DCA sub-models were added to the Evans et al. (2009) update to the Hack et al. (2006) TCE PBPK model. One-compartment models were used for DCVG and DCVC, and, based on (Kim et al. 2009b), a two-compartment model was used for DCA. Complete mathematical details and code are provided in Supplemental Material (see Supplemental Material, Details of the Bayesian PBPK modeling of TCE and its metabolites; and Supplemental Material, PBPK model code).

A hierarchical Bayesian population approach was used, as before, to estimate model parameters and their uncertainty and variability (Bois 2000; Evans et al. 2009; Hack et al. 2006). This involves specification of the hierarchical population statistical model, specification of prior distributions for model and population parameters, estimation of the posterior distributions for model parameters using Markov chain Monte Carlo (MCMC), and evaluation of convergence, the consistency of estimated parameters, and model fit. Parameter scaling relationships and prior distributions, similar to those previously reported in Chiu et al. (2009) and Evans et al. (2009), are provided in Supplemental Material, Tables S3-S6. The likelihood functions used in the Bayesian statistical analysis are described in Supplemental Material, Methods.

Previously reported population statistical models for TCE PBPK modeling (Chiu et al. 2009; Evans et al. 2009; Hack et al. 2006) did not include variability between mouse strains, and the analyses only characterized variability between studies. Because most of the previously reported data available for PBPK modeling involved only the B6C3F1 strain, most of this inter-study variability was due to variation in laboratory conditions or among studies. In order to separately characterize variation between strains, the following approach was used. For studies other than Bradford et al. (2011), only data using the B6C3F1 strain were included. For the Bradford et al. (2011) study, the B6C3F1 data (Kim et al. 2009b) were excluded. Inter-study variability (θ) in PBPK model parameters was characterized using a population model, and included for all studies. A population model for interstrain variability was constructed by adding interstrain scaling parameters (ψ) that are equal to the ratio between the PBPK model parameter for a specific strain and the PBPK model parameter for the B6C3F1 strain. Prior distributions for interstrain variability are provided in Supplemental Material, Table S5. All other aspects of the population statistical model were as reported elsewhere (Chiu et al. 2009; Evans et al. 2009).

Sensitivity analyses reported in (U.S. EPA 2011) showed that the PBPK model calibration was not sensitive to many parameters. Therefore, most of the physiological parameters and partition coefficients for which there were *in vitro* estimates available were fixed to their baseline values. The remaining parameters were estimated and evaluated using the previously reported approach (Chiu et al. 2009; Evans et al. 2009).

Results

ANOVA modeling of strain and time effects on serum concentration-time profiles of TCE metabolites

The TCE metabolite data were examined for evidence of strain and time effects using a fixed-effect two-way ANOVA model, with partial R^2 used to describe the portion of variability attributable to "strain" and "time". For strain effects, the partial R^2 may be viewed as serving as an index of heritability, although this term is used here in an approximate sense, due to the non-random sampling of strains. The overall effects of strain in the two-way model (Table 1) were highly significant for DCVG ($p = 9 \times 10^{-5}$), and not significant for TCA, DCA and DCVC. Time effects were significant for TCA, DCA, and DCVG, but not significant for DCVC. Overall, concentration-time profiling in a multistrain experimental design illustrated the importance of both strain and time on TCE metabolite concentrations. The "heritability" (partial R^2 attributable to strain) estimates ranged from 0.18 to 0.49 for all time periods (Table 1).

Interstrain variability in serum concentration-time profiles of TCE metabolites

We examined how well the Hack et al. (2006) TCE PBPK model corresponds to the concentration-time profiles of oxidative TCE metabolites in serum of B6C3F1/J mice, strain used in development of this model. A good fit was observed for the time-course TCA and DCA

concentrations (Figure 1, top panel). When compared with the kinetic data across the strains (Figure 1, bottom panel), the B6C3F1/J strain showed a peak concentration of TCA near the bottom of the distribution at 2 and 8 hours post dosing, while falling near the middle of the distribution at 24 hours. For DCA, the B6C3F1/J strain was above the distribution of plasma concentration at 2 hours while falling near the middle at 8 and 24 hours post dosing. The Monte Carlo analysis of the multistrain data (Supplemental Material, Figure S3) using the modified Hack et al. (2006) model was reasonably consistent with the range of measured concentrations of TCA at 8 and 24 hours while most measured values were below the distribution at 2 hours. For DCA, the simulations over-predicted the observed data by about a factor of two. The spread of measured concentrations for DCVG were captured by the Monte Carlo analysis at 2 hours, but with approximately 50% of the strains falling below the distribution of the simulations. The model failed to capture the rapid clearance of DCVG with all of the measured concentrations at 8 hours falling below the simulations. For DCVC, the Monte Carlo simulation was able to reasonably capture both the distribution and shape of the measured data for most strains at all three time-points.

Model refinement and Bayesian estimates of interstrain variability in serum concentration-time profiles of TCE metabolites

Because the Hack model and Monte Carlo simulations did not adequately capture the extent of interstrain variability in serum concentration-time profiles of TCE metabolites, we conducted additional model refinement using the Evans et al. (2009) update to the Hack et al. (2006) model (Figure 2), and performed Bayesian population modeling. Physiological models were added for TCA and TCOH, and a 2-compartment model was added for DCA. For the Bayesian population modeling eight independent MCMC chains were run, each to 160,000 iterations, with the first

half discarded as "burn-in" iterations. Values of the convergence diagnostic "R" were < 1.07 for all parameters, indicating convergence (less than 7% change would be expected with further simulation). Only every 500th iteration was retained to reduce autocorrelation. Therefore, a total of (8×80,000 ÷ 500) = 1,280 parameter samples were available for analysis.

Posterior distributions are summarized in Supplemental Material, Table S6. Posterior distributions for the previously developed TCE, TCA, and TCOH/TCOG sub-models were consistent with analyses of Chiu et al. (Chiu et al. 2009) and Evans et al. (Evans et al. 2009). All posteriors were well within the truncation range of the priors, so the priors were not overly constraining. Furthermore, the data appeared to be informative as to the parameters for the new DCVG, DCVC, and DCA sub-models, as evidenced by the posteriors being significantly narrower than the priors.

Figure 3 demonstrates an overall comparison of model predictions and observed data, showing that the majority of predictions are within 3-fold of the data. Individual time-courses are provided in Supplemental Material, Figures S4-S7, with predictions for the B6C3F1/J strain (Kim et al. 2009b) and two representative inbred strains DBA/2J and KK/HIJ (Bradford et al. 2011) depicted in Figures 4 and 5, respectively. We note that the most influential model refinements leading to improved predictions were the use of a two-compartment model for DCA and the change in glutathione-related parameters, specifically both increased production and increased clearance of DCVG.

Overall, model predictions are consistent with metabolism of TCE occurring predominantly by oxidation, as compared to glutathione conjugation, and with more TCA produced from oxidation

as compared to DCA. Estimates of metabolism parameters and metabolic fluxes for the B6C3F1/J mice are shown in Table 2.

Figure 6 shows PBPK model predictions for the overall flux of TCE metabolism across mouse strains. Figure 6A shows that TCA showed less interstrain variability (a 2-fold range) than DCA (a 5-fold range), though the uncertainty bounds for DCA were wider than the predicted range of variability. All strains were estimated to produce significantly more TCA than DCA; median estimates for their ratio varied from 11 to 53 (a 5-fold range of variability). Compared to B6C3F1/J, median predictions for most other strains estimated less TCA and DCA production, but with a higher TCA/DCA ratio. Figure 6B shows results for the oxidative and glutathione conjugation pathways. Less variation was predicted for oxidative metabolism (5-fold range across strains) as compared to glutathione conjugation (10-fold). Interestingly, in terms of total oxidative metabolism, all but two strains (MOLF/EiJ and 129S1/SvlmJ) were within 2-fold of each other, probably a result of blood-flow-limited metabolism. The two "outlier" strains were predicted to have notably less flux through this pathway. The B6C3F1/J strain was predicted to have more glutathione metabolism than other strains, and median estimates for the oxidation/conjugation ratio was lower than all but the 129S1/SvlmJ strain. Still, all strains were estimated to have a greater metabolic flux through oxidation as compared to glutathione conjugation; median estimates for their ratio varied about 30-fold (from 620 to 19,000).

Discussion

One of the biggest gaps in risk assessment, as identified by the National Research Council (National Research Council 2009), is that inter-individual variability is not being addressed at all (in animals), or incompletely (in epidemiological studies). There is a crucial need for the

development of approaches to estimate the quantitative impact of human inter-individual variability in personal risk from chemical exposures (Zeise et al. 2013), and with adequate human data, a number of statistical and computational tools are available to toxicologists and risk assessors (Dorne et al. 2012).

However, there are no experimental data with which to derive such population distributions for most toxicants. Some studies have been performed using data on pharmaceuticals (Hattis and Lynch 2007), but the variability in individual responses to drugs, which have generally similar pharmacokinetic properties, is unlikely to encompass the extent of variability in responses to environmental agents (Clewell et al. 2004). Epidemiological data are also of limited use because the variation in response is confounded by the variability in exposure. Combined *in vitro* and computational approaches have been proposed to characterize toxicokinetic variability (Wetmore et al. 2013), but these are limited to first-order kinetics and characterization of variability in parent compound dosimetry. Other *in vitro* approaches to evaluating the extent of and molecular mechanisms for inter-individual variability using genetically diverse cell lines have also been proposed (Lock et al. 2012; O'Shea et al. 2011). However, these and other *in vitro* approaches that do not capture the complexity of whole body toxicokinetics would not be successful for compounds such as TCE. Indeed, the metabolism of TCE is complex, with multiple metabolizing tissues and inter-organ transport, and toxicity is largely attributed to metabolites rather than the parent compound. As a consequence of these data limitations, current approaches are largely limited to applying default uncertainty factors to account for uncertainty associated with within-species variability (Stedeford et al. 2007).

One possibility to fill this gap is by characterizing the nature and quantitative extent of human variability through studies in the mouse model of the human population (Rusyn et al. 2010). Accordingly, we hypothesized that by using data from a mouse population we can build kinetic models to account for inter-individual variability in metabolism from the point of view of genetic variability. Specific focus was on PBPK modeling to generate information and kinetic parameters that may be used for verifying the models used in TCE risk assessment (Evans et al. 2009; Hack et al. 2006). In addition, a Bayesian modeling approach was used for uncertainty and sensitivity analysis (Chiu et al. 2009).

We found considerable variability in TCE metabolism across mouse strains (Bradford et al. 2011) and our novel analytical techniques offer data on additional key metabolites (Kim et al. 2009b) that were used to extend existing TCE PBPK models. While the (Hack et al. 2006) model accurately describes the kinetics of TCA in the B6C3F1/J mouse, we found that it only partially (mostly at the lower range) accounts for the variability in the toxicokinetics of TCE observed in a genetically diverse population of mouse strains. A hierarchical Bayesian approach was more successful in estimating the population variability. Using this approach, variability in the rate of production of metabolites (TCA, DCA, DCVG) was seen across strains. All strains were predicted to have a greater metabolic flux through oxidation as compared to glutathione conjugation, but with 31-fold variability in the ratio across strains (Figure 6B). While most strains had predicted total oxidative metabolism within a narrow 2-fold range, likely a result of blood-flow-limited metabolism, two strains were predicted to have notably less metabolism by this pathway. The metabolic flux through glutathione conjugation had a greater range of variability (10-fold) across strains.

These results have a number of limitations. First, the confidence intervals in some cases are quite wide, particularly for DCA. Because there is some confounding between a low rate of production and rapid clearance of DCA, both of which could account for the low levels of DCA in blood, DCA dosing would undoubtedly reduce the associated uncertainty. Additionally, it should be noted that the predominant oxidative metabolite is TCOH, which was not measured in our studies. Thus, estimating the balance of oxidation to TCOH in these strains relied on information from previous studies of B6C3F1 mice, which introduces uncertainty due to inter-study variation. Finally, many measurements of DCA, DCVC, and DCVG were near the detection limit, where analytical errors are larger, so the precision was limited by experimental variation.

We also posit that the "mouse variability distribution" may be further extrapolated to humans using the PBPK model and the resulting human variability distribution may be compared with available data on the variability of the human pharmacokinetics of TCE to determine whether the mouse derived distribution is consistent with the human evidence. Because of previous work developing human population PBPK models (Bois 2000; Chiu et al. 2009; Hack et al. 2006) a direct comparison is possible, for instance, between the extent of population variability predicted in the human population based on individual human data, and that predicted in a mouse based on multiple strain data. As shown in Table 3, where the ratio of 95th percentile and median in humans were compared with those for mouse strains, there was a remarkable correspondence between the predictions when evaluated at low doses more relevant to environmental exposures. Specifically, both the mouse and human-based analyses predicted the general trend the variability in oxidative metabolism is low (about 1.1-fold between the 95th percentile and the median), variability in TCA production is greater (about 2-fold), and variability in glutathione conjugation is the greatest (about 7-fold). Moreover, central estimates were within 20% of each

other, with the confidence intervals based on mouse data completely encompassing those based on human data. The difference in confidence intervals may simply reflect the larger number of individuals in the human analysis (n = 42) as compared to the number of strains (n = 17). It is the combination of using a PBPK model, data from the population-wide experimental model, and statistically rigorous parameter estimation that gives this approach its predictive power. These results are consistent with estimates derived from previously published analyses based on individual human data.

Thus, this case study demonstrates the feasibility of using mouse population models to characterize the nature and extent of human inter-individual variability in pharmacokinetics for toxicologically relevant measures of internal dose – a similar approach that could be applied to other chemicals. As characterization of pharmacokinetic variability is a necessary precursor to characterization of pharmacodynamic variability, this work considerably extends the utility of the PBPK modeling tools and Bayesian population analysis to population-wide data, both in immediate impact and in future translational potential for risk assessment.

References

Bois FY. 2000. Statistical analysis of Clewell et al. PBPK model of trichloroethylene kinetics. Environ Health Perspect 108 Suppl 2:307-316.

Bradford BU, Lock EF, Kosyk O, Kim S, Uehara T, Harbourt D, et al. 2011. Interstrain differences in the liver effects of trichloroethylene in a multistrain panel of inbred mice. Toxicol Sci 120(1):206-217.

Chiu WA, Jinot J, Scott CS, Makris SL, Cooper GS, Dzubow RC, et al. 2013. Human health effects of trichloroethylene: key findings and scientific issues. Environ Health Perspect 121(3):303-311.

Chiu WA, Okino MS, Evans MV. 2009. Characterizing uncertainty and population variability in the toxicokinetics of trichloroethylene and metabolites in mice, rats, and humans using an updated database, physiologically based pharmacokinetic (PBPK) model, and Bayesian approach. Toxicol Appl Pharmacol 241(1):36-60.

Clewell HJ, Gentry PR, Covington TR, Sarangapani R, Teeguarden JG. 2004. Evaluation of the potential impact of age- and gender-specific pharmacokinetic differences on tissue dosimetry. Toxicol Sci 79(2):381-393.

Dorne JL, Amzal B, Bois F, Crepet A, Tressou J, Verger P. 2012. Population effects and variability. Methods Mol Biol 929:521-581.

Evans MV, Chiu WA, Okino MS, Caldwell JC. 2009. Development of an updated PBPK model for trichloroethylene and metabolites in mice, and its application to discern the role of oxidative metabolism in TCE-induced hepatomegaly. Toxicol Appl Pharmacol 236(3):329-340.

Guha N, Loomis D, Grosse Y, Lauby-Secretan B, El Ghissassi F, Bouvard V, et al. 2012. Carcinogenicity of trichloroethylene, tetrachloroethylene, some other chlorinated solvents, and their metabolites. Lancet Oncol 13(12):1192-1193.

Hack CE, Chiu WA, Jay ZQ, Clewell HJ. 2006. Bayesian population analysis of a harmonized physiologically based pharmacokinetic model of trichloroethylene and its metabolites. Regul Toxicol Pharmacol 46(1):63-83.

Hattis D, Lynch MK. 2007. Empirically observed distributions of pharmacokinetic and pharmacodynamic variability in humans-Implications for the derivation of single point component uncertainty factors providing equivalent protection as existing RfDs. In: Toxicokinetics in Risk Assessment, (Lipscomb JC, Ohanian EV, eds):Informa Healthcare, USA, Inc., 69-93.

Kim S, Collins LB, Boysen G, Swenberg JA, Gold A, Ball LM, et al. 2009a. Liquid chromatography electrospray ionization tandem mass spectrometry analysis method for simultaneous detection of trichloroacetic acid, dichloroacetic acid, S-(1,2-dichlorovinyl)glutathione and S-(1,2-dichlorovinyl)-L-cysteine. Toxicology 262(3):230-238.

Kim S, Kim D, Pollack GM, Collins LB, Rusyn I. 2009b. Pharmacokinetic analysis of trichloroethylene metabolism in male B6C3F1 mice: Formation and disposition of trichloroacetic acid, dichloroacetic acid, S-(1,2-dichlorovinyl)glutathione and S-(1,2-dichlorovinyl)-L-cysteine. Toxicol Appl Pharmacol 238(1):90-99.

Lash LH, Fisher JW, Lipscomb JC, Parker JC. 2000. Metabolism of trichloroethylene. Environ Health Perspect 108 Suppl 2:177-200.

Lock EF, Abdo N, Huang R, Xia M, Kosyk O, O'Shea SH, et al. 2012. Quantitative high-throughput screening for chemical toxicity in a population-based in vitro model. Toxicol Sci 126(2):578-588.

National Research Council. 2006. Assessing the Human Health Risks of Trichloroethylene: Key Scientific Issues Washigton, DC: The National Academies Press.

National Research Council. 2009. Science and Decisions: Advancing Risk Assessment. Washington, DC: National Academies Press.

O'Shea SH, Schwarz J, Kosyk O, Ross PK, Ha MJ, Wright FA, et al. 2011. In vitro screening for population variability in chemical toxicity. Toxicol Sci 119(2):398-407.

Rusyn I, Gatti DM, Wiltshire T, Kleeberger SR, Threadgill DW. 2010. Toxicogenetics: population-based testing of drug and chemical safety in mouse models. Pharmacogenomics 11(8):1127-1136.

Stedeford T, Zhao QJ, Dourson ML, Banasik M, Hsu CH. 2007. The application of non-default uncertainty factors in the U.S. EPA's Integrated Risk Information System (IRIS). Part I: UF(L), UF(S), and "other uncertainty factors". J Environ Sci Health C Environ Carcinog Ecotoxicol Rev 25(3):245-279.

U.S. EPA. 2011. Toxicological Review of Trichloroethylene (CAS No. 79-01-6): In Support of Summary Information on the Integrated Risk Information System (IRIS). EPA/635/R-09/011F. Washington, DC.

Wetmore BA, Wambaugh JF, Ferguson SS, Li L, Clewell HJ, 3rd, Judson RS, et al. 2013. Relative impact of incorporating pharmacokinetics on predicting in vivo hazard and mode of action from high-throughput in vitro toxicity assays. Toxicol Sci 132(2):327-346.

Zeise L, Bois FY, Chiu WA, Hattis D, Rusyn I, Guyton KZ. 2013. Addressing human variability in next-generation human health risk assessments of environmental chemicals. Environ Health Perspect 121(1):23-31.

Table 1. Results of ANOVA modeling of the effect of time and strain on TCE metabolite concentrations in mouse serum.

Metabolite	Time point (hr)	Sample size	Partial R^2 ("heritability")	Strain: F	Strain: p-value	Time: F	Time: p-value
TCA	2	37	0.25	0.53	0.890		
	8	36	0.63	2.51	0.028		
	24	23	0.76	2.65	0.066		
	All		0.18	1.24	0.263	59.00	<1E-10
DCA	2	38	0.56	2.13	0.052		
	8	36	0.58	2.09	0.061		
	24	25	0.78	2.53	0.073		
	All		0.22	1.69	0.075	6.19	0.003
DCVG	2	36	0.82	6.62	0.00001		
	8	33	0.89	8.88	<1E-10		
	24	12	1.00	1376	0.021		
	All		0.49	3.75	0.00009	40.50	<1E-10
DCVC	2	32	0.60	1.83	0.118		
	8	19	0.72	1.27	0.404		
	24	8	0.74	0.48	0.801		
	All		0.34	1.41	0.189	1.53	0.229

Table 2. TCE metabolism parameters for B6C3F1/J strain: median (2.5%, 97.5%) of posterior distribution.

Parameter or prediction	**Abbreviation**	**Value**
VMax for liver oxidation (mg/hr)	VMax	2.1 (0.73, 5.6)
KM for liver oxidation (mg/L)	KM	3.3 (0.63, 19)
VMax for liver GSH conjugation (mg/hr)	VMaxDCVG	0.006 (0.003, 5.9)
KM for liver GSH conjugation (mg/L)	KMDCVG	0.06 (0.003, 9.8e4)
VMax/KM for liver GSH conjugation (L/hr)	Vmax/KM	0.1 (4e-5, 2.1)
Dose (mg) [fixed]		76.4
Amount of TCE metabolized (mg)	AMetOx	16 (5.5, 60)
Amount of TCE conjugated (mg)	AMetGSH	0.05 (0.03, 0.5)
Amount of TCA produced (mg)	TotTCAProd	3.4 (1.4, 15)
Amount of DCA produced (mg)	TotDCAProd	0.3 (0.02, 3.7)
Oxidation/GSH ratio (mg TCE oxidized/mg TCE conjugated)	OXtoGSHRatio	290 (41, 1070)
TCA/DCA ratio (mmol TCA produced/mmol DCA produced)	TCAtoDCAratio	10 (0.9, 130)

Table 3. Comparison of Chiu et al. (2009) human variability predictions for TCE metabolism with variability predictions for TCE metabolism among mouse strains. Ratios of 95th percentile/50th percentile individual or strain are shown. Median estimate and 95% confidence interval were calculated at an oral dose of 0.001 mg/(kg d), where non-linearities in toxicokinetics are negligible.

Parameter	**Human inter-individual variability (Chiu et al. 2009)**	**Mouse interstrain variability (present analysis)**
TCE oxidized by P450	1.11 (1.05, 1.22)	1.05 (1.01, 1.27)
Total TCA produced	2.09 (1.81, 2.51)	1.77 (1.36, 2.99)
TCE conjugated with glutathione	6.61 (3.95, 11.17)	7.12 (3.43, 20.66)

Figure Legends

Figure 1. Top panel, Hack et al. (2006) TCE PBPK model simulation of TCA and DCA compared to the measured data [from (Kim et al. 2009b)] for the B6C3F1/J strain which was used in the original model development. Bottom panel, fits to TCA and DCA data [from (Bradford et al. 2011)] from a panel of inbred mouse stains.

Figure 2. Schematic of the mouse PBPK model of TCE and its metabolites. The image has been modified from Chiu et al. (2009).

Figure 3. Global evaluation of model fit, comparing toxicokinetic data (x-axis) and PBPK model predictions (y-axis), each with 95% confidence intervals. In some cases, the confidence interval on the data included 0, as indicated by horizontal error bars that extend all the way to the left. The solid grey diagonal line indicates where data and predictions are equal, and the dotted lines indicate where they are within 3-fold.

Figure 4. Comparison of data (solid boxes with ±1 SD error bars) and PBPK model predictions (solid lines: interquartile range; grey area: 95% confidence interval) for TCE metabolites in B6C3F1 mice [data from (Kim et al. 2009b)].

Figure 5. (A) Hierarchical population statistical model for PBPK model uncertainty and variability. Square nodes denote fixed or observed quantities; circle nodes represent uncertain or unobserved quantities, and the PBPK model outputs are denoted by the inverted triangle. Solid arrows denote a stochastic relationship represented by a conditional distribution [A→B means B~P(B|A)], while dashed arrows represent a functional relationship [B = f(A)]. The population consists of studies i, each of which contains experiments or strains j, with exposure parameters

E_{ij}, and data y_{ij} collected at times t_{ij}. The PBPK model produces outputs f_{ij}. The difference between data and predictions is assumed to have a distribution with variance σ^2, which is assigned a prior distribution (Pr). The PBPK model uses non-strain-specific parameters θ_i, measured covariates φ_i, and strain-specific parameters ψ_j. The parameters are each drawn from population distributions with mean $M_{\theta \text{ or } \psi}$ and variance $V_{\theta \text{ or } \psi}$, each of which are in turn assigned prior distributions. **(B)** Comparison of data (solid boxes with ±1 SD error bars) and PBPK model predictions (solid lines: interquartile range; grey area: 95% confidence interval) for two representative mouse inbred strains [data from (Bradford et al. 2011)].

Figure 6. Predictions for TCE metabolites and metabolite fluxes across mouse strains (median and 95% confidence interval). **(A)** TCA produced, DCA produced, and the ratio of TCA/DCA produced. **(B)** Flux of TCE metabolism through oxidation, flux through glutathione conjugation, and ratio of oxidation to glutathione conjugation.

Figure 1.

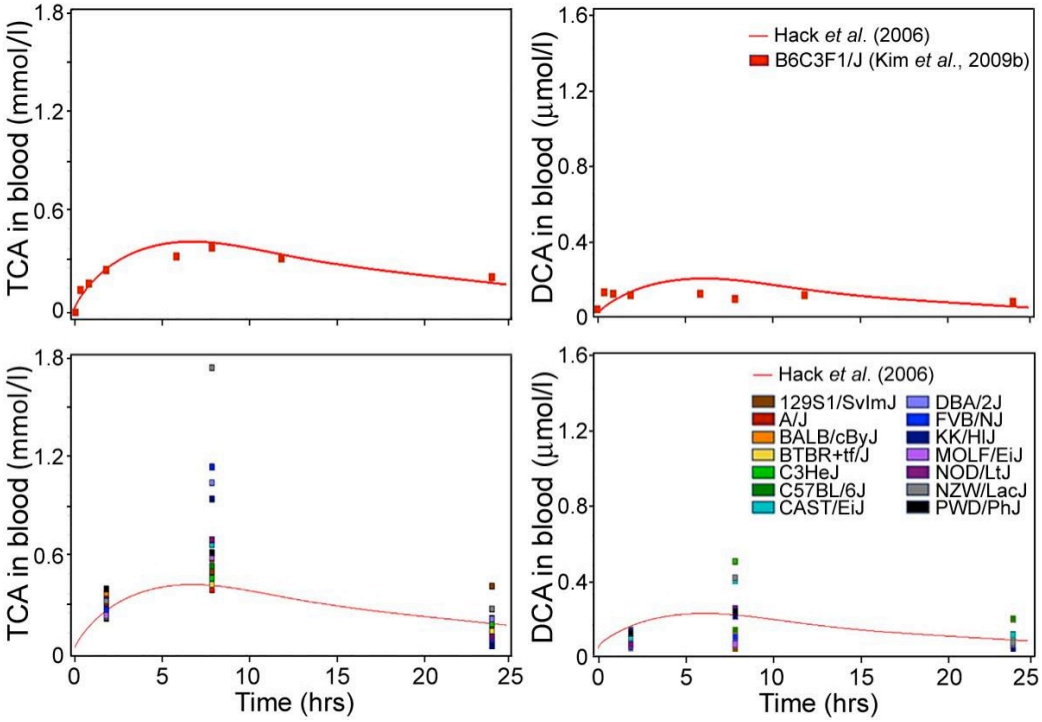
TCA in blood (mmol/l)
DCA in blood (µmol/l)
Hack et al. (2006)
B6C3F1/J (Kim et al., 2009b)
Hack et al. (2006)
129S1/SvImJ
A/J
BALB/cByJ
BTBR+tf/J
C3HeJ
C57BL/6J
CAST/EiJ
DBA/2J
FVB/NJ
KK/HlJ
MOLF/EiJ
NOD/LtJ
NZW/LacJ
PWD/PhJ
Time (hrs)

Figure 2.

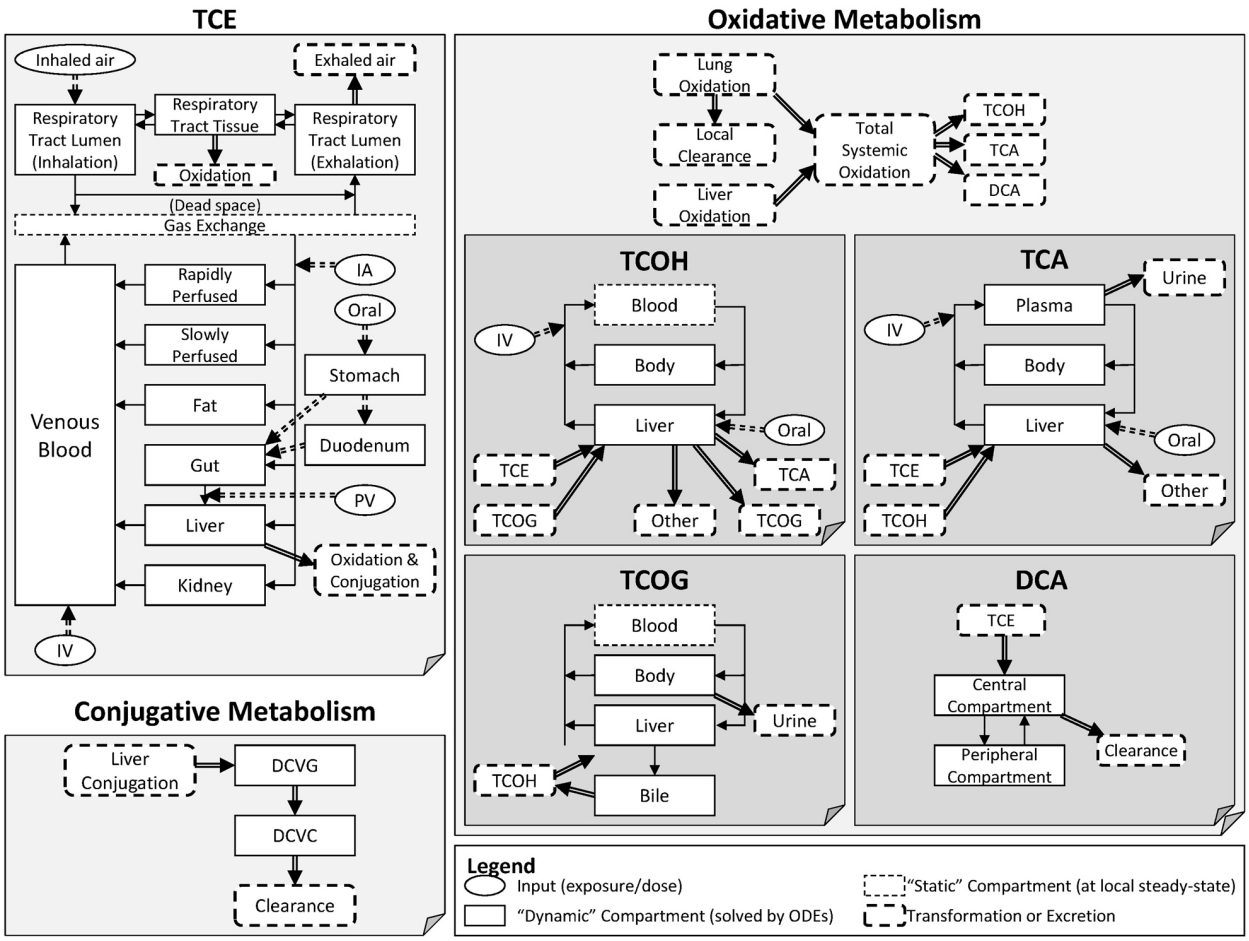
TCE
Inhaled air
Exhaled air
Respiratory Tract Lumen (Inhalation)
Respiratory Tract Tissue
Respiratory Tract Lumen (Exhalation)
Oxidation
(Dead space)
Gas Exchange
Venous Blood
Rapidly Perfused
Slowly Perfused
Fat
Gut
Liver
Kidney
IA
Oral
Stomach
Duodenum
PV
Oxidation & Conjugation
IV
Oxidative Metabolism
Lung Oxidation
Local Clearance
Liver Oxidation
Total Systemic Oxidation
TCOH
TCA
DCA
TCOH
Blood
Body
Liver
IV
Oral
TCE
TCA
TCOG
Other
TCOG
TCA
Plasma
Urine
Body
Liver
IV
Oral
TCE
Other
TCOH
TCOG
Blood
Body
Liver
Urine
TCOH
Bile
DCA
TCE
Central Compartment
Peripheral Compartment
Clearance
Conjugative Metabolism
Liver Conjugation
DCVG
DCVC
Clearance
Legend
Input (exposure/dose)
"Dynamic" Compartment (solved by ODEs)
"Static" Compartment (at local steady-state)
Transformation or Excretion

Figure 3.

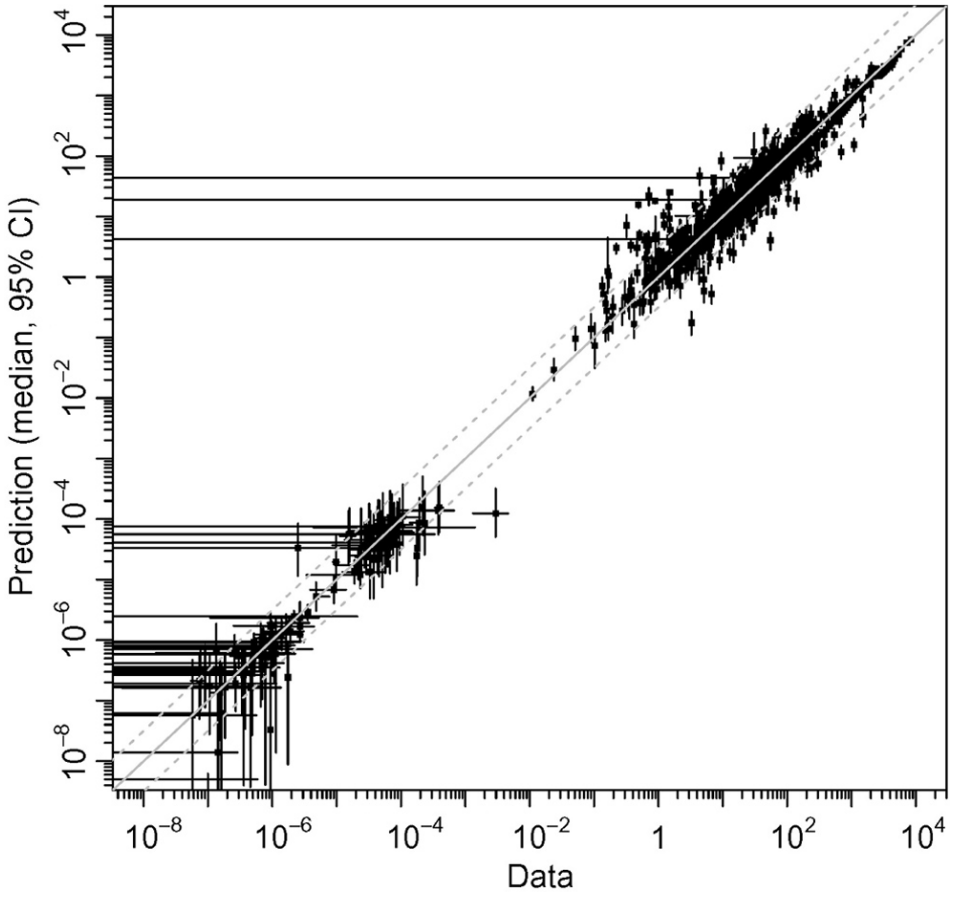

Figure 4.

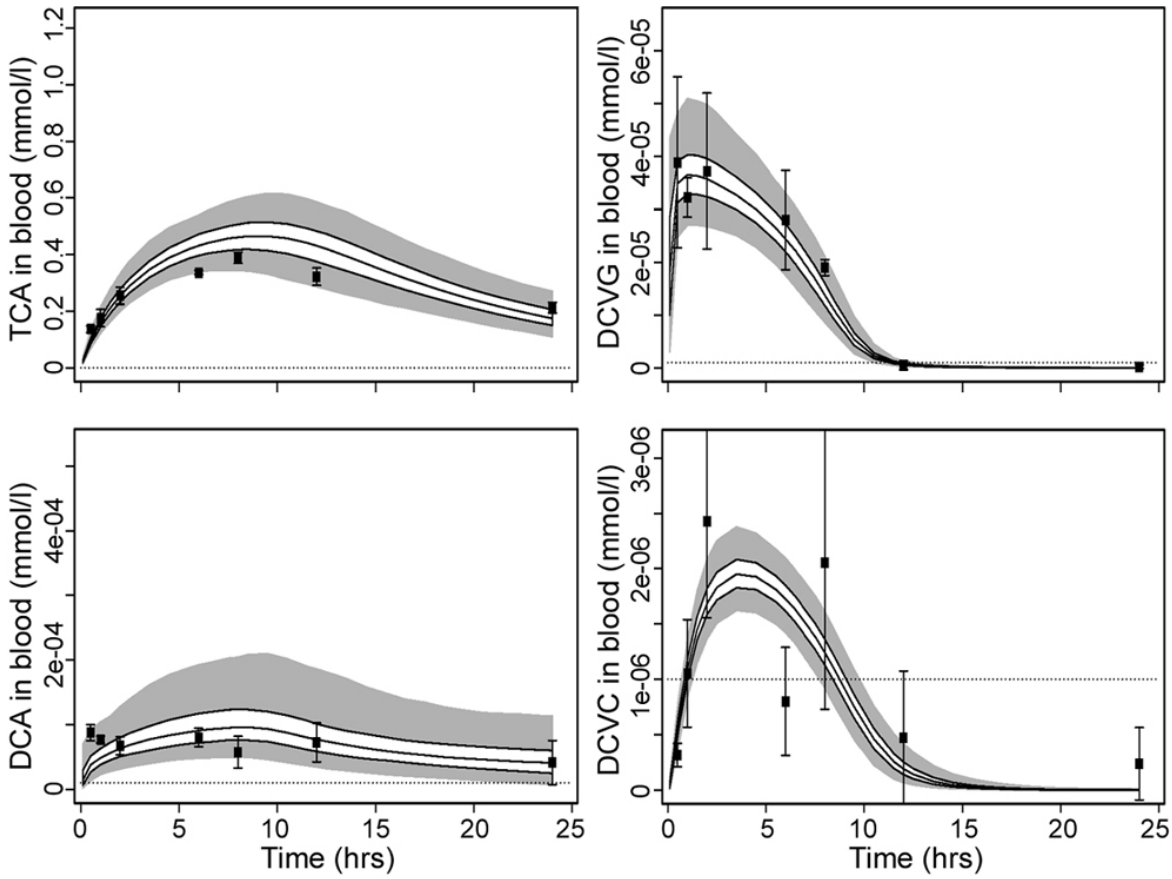
TCA in blood (mmol/l)
0
0.2
0.4
0.6
0.8
1.0
1.2
DCVG in blood (mmol/l)
0
2e-05
4e-05
6e-05
DCA in blood (mmol/l)
0
2e-04
4e-04
DCVC in blood (mmol/l)
0
1e-06
2e-06
3e-06
0
5
10
15
20
25
Time (hrs)
Time (hrs)

Figure 5.

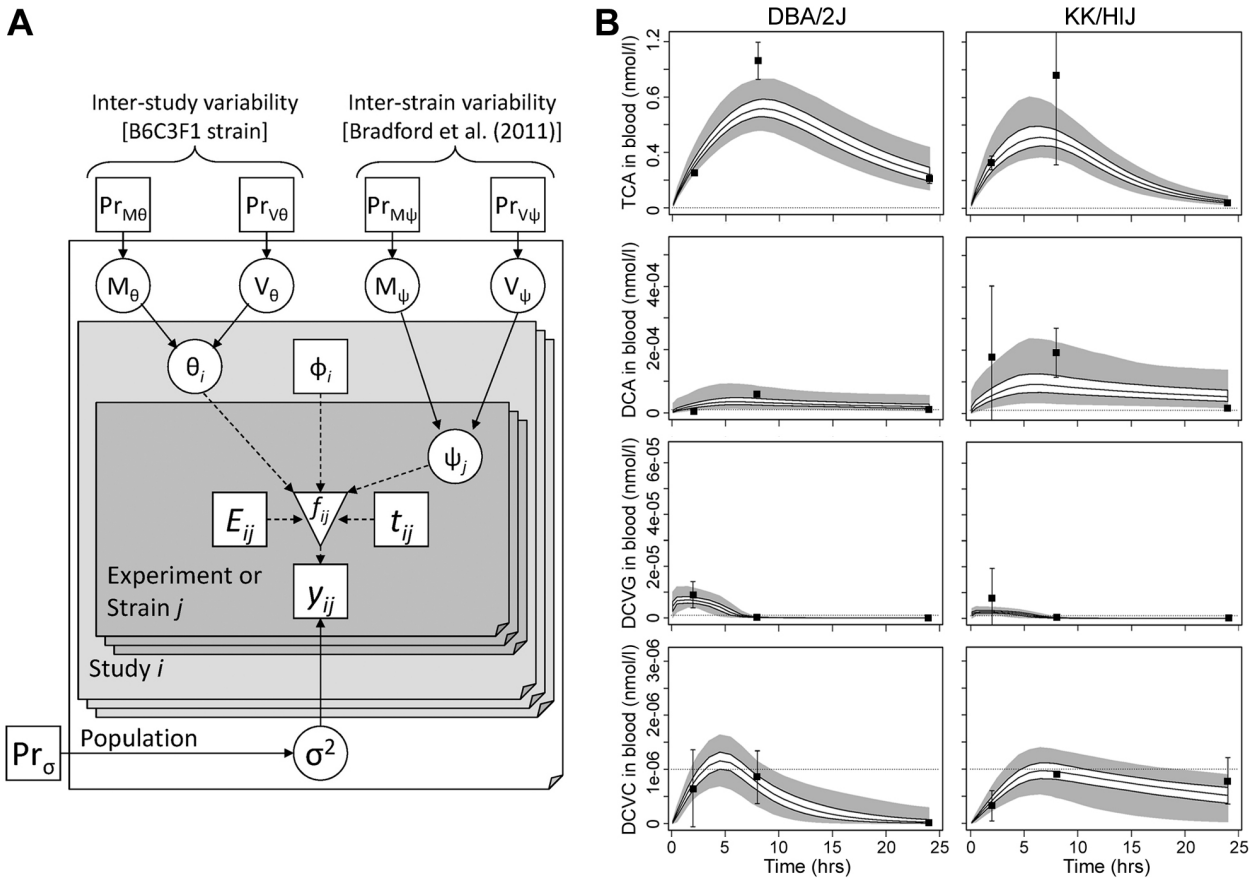
A
Inter-study variability
[B6C3F1 strain]
Inter-strain variability
[Bradford et al. (2011)]
Experiment or
Strain j
Study i
Population
B
DBA/2J
KK/HIJ
TCA in blood (nmol/l)
DCA in blood (nmol/l)
DCVG in blood (nmol/l)
DCVC in blood (nmol/l)
Time (hrs)
Time (hrs)

Figure 6.

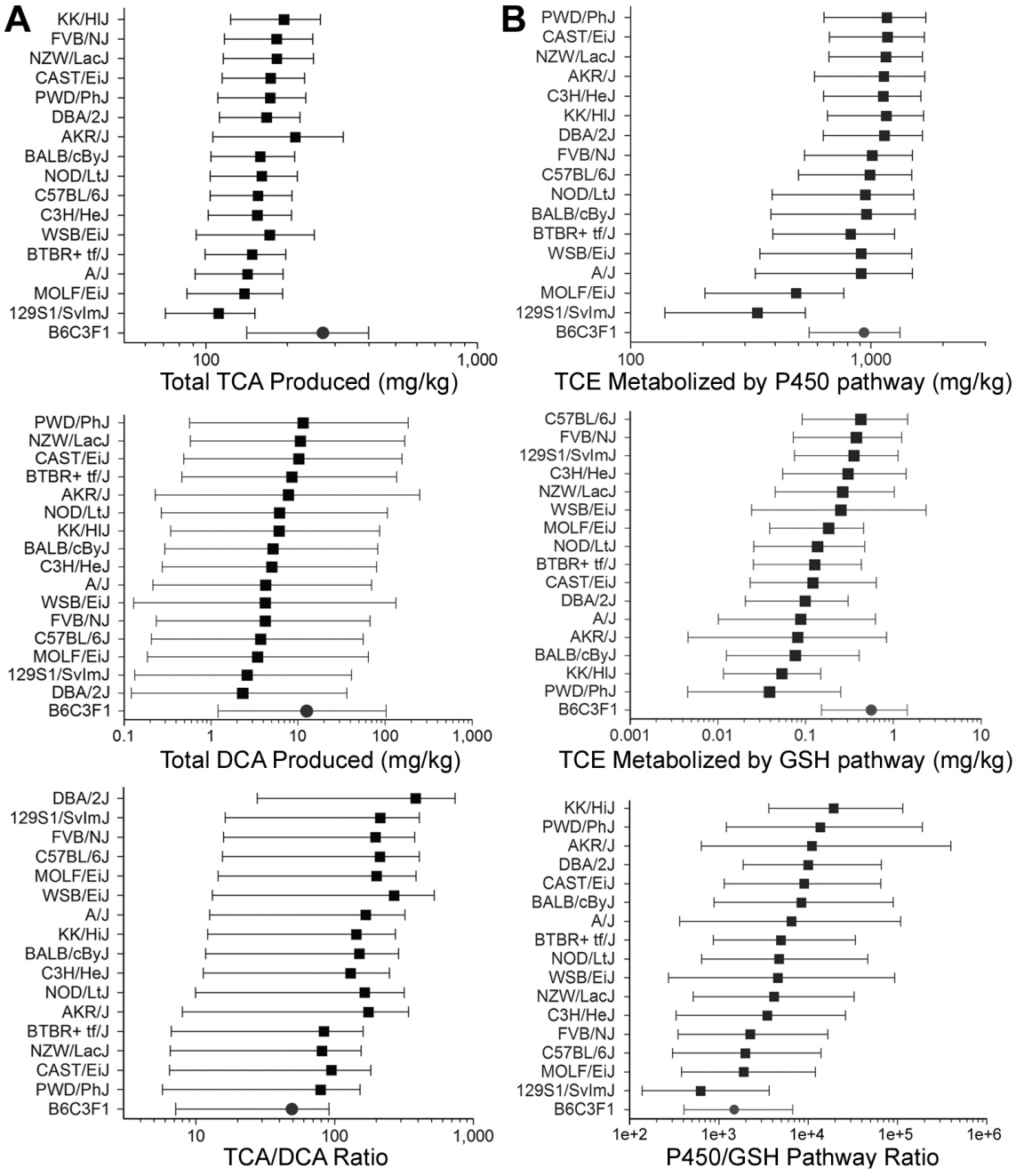
A
KK/HlJ
FVB/NJ
NZW/LacJ
CAST/EiJ
PWD/PhJ
DBA/2J
AKR/J
BALB/cByJ
NOD/LtJ
C57BL/6J
C3H/HeJ
WSB/EiJ
BTBR+ tf/J
A/J
MOLF/EiJ
129S1/SvImJ
B6C3F1
100
1,000
Total TCA Produced (mg/kg)
B
PWD/PhJ
CAST/EiJ
NZW/LacJ
AKR/J
C3H/HeJ
KK/HlJ
DBA/2J
FVB/NJ
C57BL/6J
NOD/LtJ
BALB/cByJ
BTBR+ tf/J
WSB/EiJ
A/J
MOLF/EiJ
129S1/SvImJ
B6C3F1
100
1,000
TCE Metabolized by P450 pathway (mg/kg)
PWD/PhJ
NZW/LacJ
CAST/EiJ
BTBR+ tf/J
AKR/J
NOD/LtJ
KK/HlJ
BALB/cByJ
C3H/HeJ
A/J
WSB/EiJ
FVB/NJ
C57BL/6J
MOLF/EiJ
129S1/SvImJ
DBA/2J
B6C3F1
0.1
1
10
100
1,000
Total DCA Produced (mg/kg)
C57BL/6J
FVB/NJ
129S1/SvImJ
C3H/HeJ
NZW/LacJ
WSB/EiJ
MOLF/EiJ
NOD/LtJ
BTBR+ tf/J
CAST/EiJ
DBA/2J
A/J
AKR/J
BALB/cByJ
KK/HlJ
PWD/PhJ
B6C3F1
0.001
0.01
0.1
1
10
TCE Metabolized by GSH pathway (mg/kg)
DBA/2J
129S1/SvImJ
FVB/NJ
C57BL/6J
MOLF/EiJ
WSB/EiJ
A/J
KK/HiJ
BALB/cByJ
C3H/HeJ
NOD/LtJ
AKR/J
BTBR+ tf/J
NZW/LacJ
CAST/EiJ
PWD/PhJ
B6C3F1
10
100
1,000
TCA/DCA Ratio
KK/HiJ
PWD/PhJ
AKR/J
DBA/2J
CAST/EiJ
BALB/cByJ
A/J
BTBR+ tf/J
NOD/LtJ
WSB/EiJ
NZW/LacJ
C3H/HeJ
FVB/NJ
C57BL/6J
MOLF/EiJ
129S1/SvImJ
B6C3F1
1e+2
1e+3
1e+4
1e+5
1e+6
P450/GSH Pathway Ratio